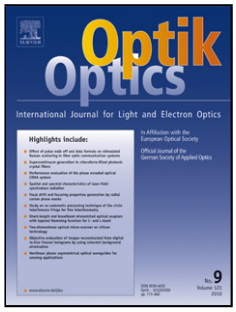

Title: Three-dimensional planar object tracking with sub-pixel accuracy

Author: A.B. Roig J. Espinosa J. Perez B. Ferrer D. Mas

PII: S0030-4026(15)00542-2
DOI: http://dx.doi.org/doi:10.1016/j.ijleo.2015.06.070
Reference: IJLEO 55705

To appear in:

Received date: 8-5-2014
Accepted date: 26-6-2015

Please cite this article as: A.B. Roig, J. Espinosa, J. Perez, B. Ferrer, D. Mas, Three-dimensional planar object tracking with sub-pixel accuracy, *Optik - International Journal for Light and Electron Optics* (2015), http://dx.doi.org/10.1016/j.ijleo.2015.06.070

Three-dimensional planar object tracking with sub-pixel accuracy

A.B. Roig, J. Espinosa, J. Perez, B. Ferrer*, D. Mas

Inst. Fisica Aplicada a las Ciencias y Tecnologías , University of Alicante,PO Box 99, 03080 Alicante (SPAIN)

**Dep. Ing. Construccion, University of Alicante, PO Box 99, 03080 Alicante (SPAIN)*

ABSTRACT

Subpixel techniques are commonly used to increase the spatial resolution in tracking tasks. Object tracking with targets of known shape permits obtaining information about object position and orientation in the three-dimensional space. A proper selection of the target shape allows us to determine its position inside a plane and its angular and azimuthal orientation under certain limits. Our proposal is demonstrated both numerical and experimentally and provides an increase the accuracy of more than one order of magnitude compared to the nominal resolution of the sensor. The experiment has been performed with a high-speed camera, which simultaneously provides high spatial and temporal resolution, so it may be interesting for some applications where this kind of targets can be attached, such as vibration monitoring and structural analysis.

Keywords Target tracking, shape detection, subpixel techniques, high speed camera.

Corresponding author:

David Mas (david.mas@ua.es)

Ph: +34 965 903 400

Fax: +34 965 903 464

1. Introduction

Computer vision can be defined as the science and technology of machines that are able to see, which means that machines can extract information from images. Among many other applications, computer vision systems are used for object segmentation and tracking [1], and cover tasks from simple presence detection to non-invasive detection of small movements [2].

Precise tracking of fast moving objects usually requires high temporal and spatial resolution. Unfortunately, spatial resolution of sensors is strongly linked to the processing speed. Due to hardware limitations, CCDs and CMOS sensors are unable to simultaneously acquire, process and store large amount of data, thus impeding recording large video sequences at very high speeds. Therefore, if temporal resolution is priorized, spatial resolution has to be reduced in order to maintain the data-transfer rate.

Apart from the loss of fine image details, reduced spatial resolution also limits the accuracy in the detection tasks. Notice that motion is detected by changes in the excited pixels so, the less and larger the pixels are, the less detection accuracy is obtained. Depending on the particular application, improving the spatial resolution of the camera may be uneconomical or even impractical. However, one can take advantage of some "a priori" information about the system and the target to be tracked and, afterwards, use image processing techniques to increase the performance of the system. These methods are knowns as subpixel techniques.

Although there are alternate theoretical proposals [3], the most common methods for subpixel object tracking consist of smart interpolation of image features and it can be done in both spatial and frequency domain. In [4,5], the authors summarize the different methods for target recognition and location. From both tasks, target recognition is the most complicated since it requires of a proper analysis and segmentation of the target from the whole scene. This process can be simplified and accelerated by using specific targets that are easy to recognize. Among all possible targets, elliptical objects (including circles) are usually preferred since its shape is preserved under lateral shifts and rotations [6,7].

The first step of all algorithms for the object location in a scene consists of target isolation from the background image, which allows obtaining a distinguishable "blob" object. This step is usually performed through binary thresholding, hard-clipping or edge extraction. Once the target is isolated, several techniques can be applied for subpixel location of the blob [4,7,8]. Among them, those based on centroid calculation seem to be the most accurate and reliable methods. Unfortunately, the method is very sensitive to illumination conditions and its accuracy can be compromised in presence of noise and uneven or changing illumination [7]. Other methods based on image intensity, like those based on image correlation or template matching, may be affected of similar problems [9]. These drawbacks become more evident under the particular characteristics of image sequences obtained from fast cameras since acquisition at high frame rates needs of low exposition (typically few milliseconds), so captured images suffer from low contrast and high noise-level.

The methods based on the detection and fitting of a contour are a reliable and robust alternative for object tracking. Their performance may not be as good as centroid-based techniques when dealing with static images under ideal conditions. Nevertheless, for dynamic scenes or non-controlled illumination, contour based methods are more robust since irregularities in the object shape can be detected and controlled through the mean squared error of the fitting. Additionally, they can provide information about the target geometry that may be interesting in case of shape changes.

Three dimensional object tracking adds an additional difficulty to the problem since targets may change not only their position but also their shape [12]. Therefore, limiting the object geometry and the movement degrees of freedom will facilitate the tracking task. Furthermore, algorithms will be faster and easier to implement. We propose to use a planar object of known geometry and with restricted movements as target, so detection and movement tracking leads to straightforward algorithms. It consists of a high-contrast elliptical line. Its geometrical parameters can be used to determine both the target position and orientation. Although the imposed restrictions limit the applicability of the method, there still is a wide range of situations where it can be used. In our case, we are interested in fields as different as structural vibrations [11] or eye tracking [2], where the object movement is clearly restricted.

Numerical simulations presented in Section 3 prove that the methods and targets used permit increased resolution since the accuracy obtained can be better than 0.03 px for displacement tracking, 0.05º for in-plane rotations and 0.1 px for axes length change. The experimental results in Section 4 show that noise, reduced contrast and other factors decrease the accuracy to 0.2 px, 0.1º and 0.3 px, respectively. Tracking accuracy is in consonance with other authors' results [7]. However, references for accuracy for tracking rotation and shape changes could not be found in the literature. Additionally, the method does not require of additional cameras or previous calibration of the imaging system [14], which makes it fast and simple to implement.

2. Method

The proposed method is simple and it briefly consists of fitting the contour of a registered blob to a known mathematical expression. Therefore, it is necessary to select a target that provides a convenient contour line. Among all possible targets, the most appropriate are those preserving the topology at all possible movements [6]. The simplest one fulfilling this characteristic is an ellipse with general equation

$$Ax^2 + Bxy + Cy^2 + Dx + Ey + F = 0 \tag{1}$$

By least squares fitting the blob contour to equation (1), we obtain several geometrical parameters of the ellipse, such as center (x_c, y_c), long and short axes (a, b), and orientation, θ [14]:

$$(x_c, y_c) = \left(\frac{-D}{2A}, \frac{-E}{2C}\right) \tag{2}$$

$$a = 2\max\left[\sqrt{\frac{D^2}{4A^2}+\frac{E^2}{4AC}-\frac{F}{A}}, \sqrt{\frac{D^2}{4AC}+\frac{E^2}{4C^2}-\frac{F}{C}}\right]$$

$$b = 2\min\left[\sqrt{\frac{D^2}{4A^2}+\frac{E^2}{4AC}-\frac{F}{A}}, \sqrt{\frac{D^2}{4AC}+\frac{E^2}{4C^2}-\frac{F}{C}}\right] \quad (3)$$

$$\theta = \frac{1}{2}\arctan\left(\frac{B}{C-A}\right) \quad (4)$$

The center of the ellipse locates the object inside the image plane. Orientation of the ellipse informs about object rotations in the image plane, whereas the axis lengths may both be associated to real changes in the ellipse shape (deformations) or provide information about rotations around an axis contained in the image plane. This kind of movements will be seen as a change in the perspective and, consequently, in the apparent eccentricity.

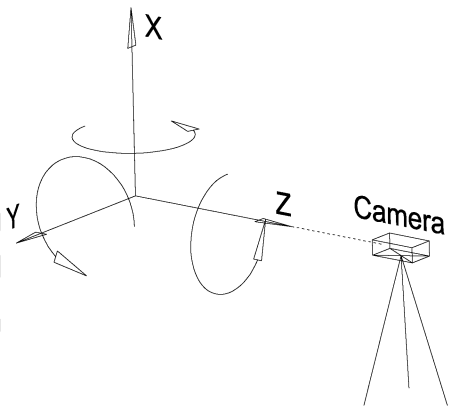

Figure 1. *Possible movements of an object in the space (three shifts and three rotations). Our method allows reporting five of the six possibilities, just loosing displacement along the camera axis (z-axis) due to the constancy of axial magnification.*

The movement of a solid object in the three-dimensional space can be decomposed in six basic movements: three shifts and three rotations around the coordinate axes. The geometrical parameters in equations (2-4) report on five of these six basic object movements: two shifts and three rotations around the coordinate axes (see figure 1). The missing shift corresponds to

movements in the direction perpendicular to the image plane, which are not detectable unless they provoke a noticeable change in the object size.

The easiest case for object tracking happens when the target is attached to the object under study and a video sequence is registered. Therefore, contrast is good and the target is relatively free of noise. Nevertheless, round shapes are very common in natural scenes and thus, the method can be applied on specific details whose contour can be assumed to be elliptical. Notice that, in all cases, accurate focusing of the target is not indispensable since the unique requirement is a contour detection. The tracking is performed by fitting to (1) the contour from each frame of the sequence. All these parameters can be calculated with subpixel accuracy, which increases the nominal resolution of the sensor.

3. Numerical simulations

The accuracy of the method has been tested through several numerical simulations. The aim is to determine the sensitivity of the contour fitting to detect subpixel changes in the ellipse parameters in ideal conditions. Thus, we have calculated the response to center displacement, shape variation (axis length) and change in the orientation of the ellipse for different target sizes. Several elliptical contours have been implemented on a discrete mesh through software and then least square fitted to (1) in order to obtain the parameters from eq. (2) to (4).

The first simulation concerns displacement tracking. Circular targets of diameters ranging from 4 to 400 px have been displaced one full pixel in 100 steps. We compare theoretical center positions with those computed through eq. (2) and obtain the error for each incremental sequence. In figure 2, we represent the maximum error, the mean error and its standard deviation of the whole movement sequence for each target diameter.

Small sizes present the strongest error oscillations. This effect is due to the discrete nature of the target. In those cases, the target is strongly pixelated and it may change its shape with the displacement [14]. As the target gets larger, the discrete shape becomes more close to the

analytical case and the error decreases. For diameters larger than 100 px, the maximum error in position determination is below 0.05 px and it slowly decreases with the size, being even lower than 0.025 px for target sizes above 250 px.

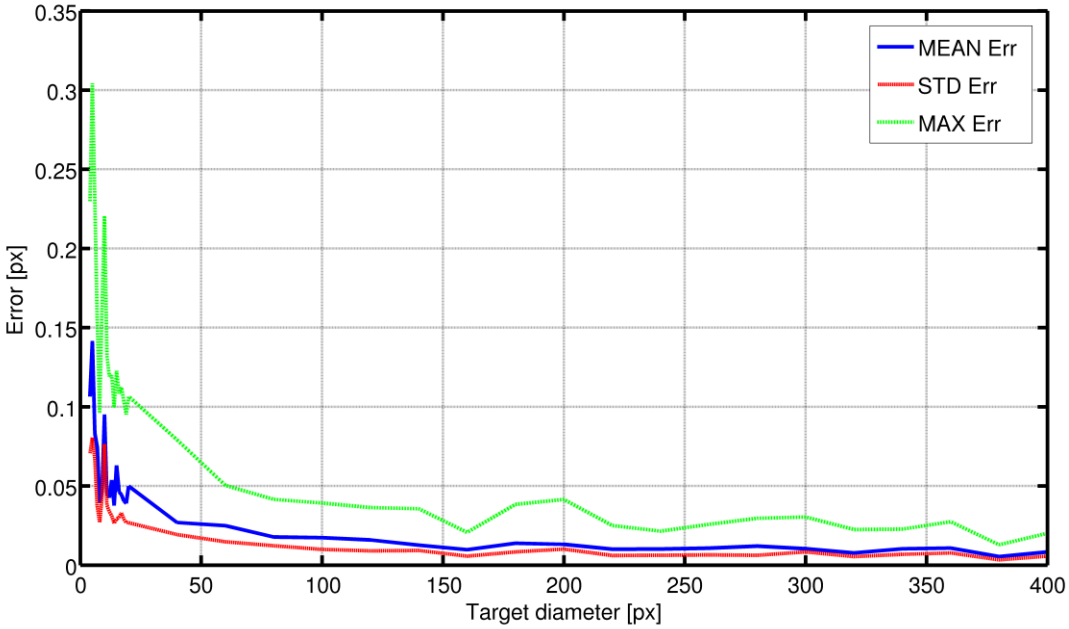

Figure 2. *Accuracy of target center location for several circle sizes. Lines represent the mean error in determining the exact position, the standard deviation and the maximum error.*

In figure 3, we analyze the accuracy of the method in detecting changes in the ellipse shape. We have selected an ellipse with the vertical axis equal to 80 px and the horizontal one has been varied from 4 to 400 px. Now, we focus in the analysis of the sensitivity of the method to a full pixel change in the horizontal axis in steps of 0.01 px. As above, the maximum, mean and standard deviation of the axis estimated error has been evaluated.

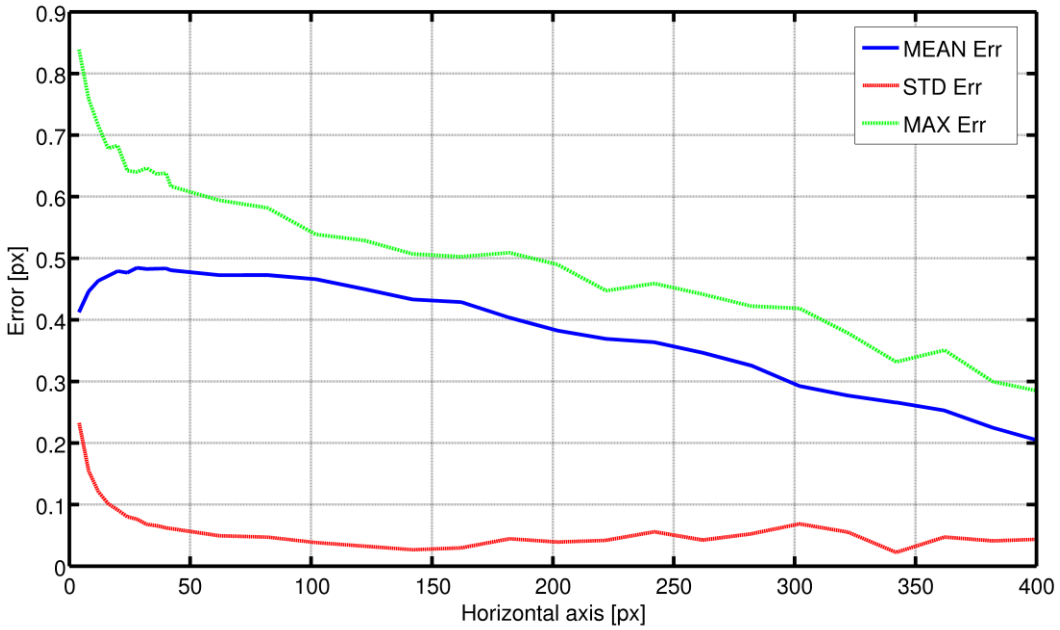

Figure 3. *Accuracy of axis-size determination for several elliptic targets. The vertical axis has been fixed to 80 px while the horizontal one has been changed to different lengths. Lines represent the mean error in determining the axis size, the standard deviation and the maximum error.*

We can appreciate that the determination of the axis length is not very accurate although subpixel accuracy is obtained. It is noticeable that the more eccentric the ellipse is, the better accuracy is obtained. We would like to point out that both the mean difference and the maximum error are relatively high, whereas the standard deviation is low and almost constant. This means that, although the absolute value of the parameter is not properly obtained, dispersion is really low, thus pointing to a zero-bias error.

Note that, in many applications, only relative changes are needed. In that case, the accuracy of the method is not determined by the maximum absolute error but by the dispersion of the measurement. Thus, we take three times the standard deviation of the error in order to determine the maximum error variation. In this case, this criterion leads to a precision of 0.15 px, although the error in the absolute determination of the axis length is above 0.3 px.

Finally, we have checked the capability of our proposal to track target orientations (in-plane rotations). We have taken the same set of targets from the previous test: ellipses with the vertical axis equal to 80 px and the horizontal ranging from 4 to 400 px (figure 4). Each ellipse is rotated 1º clockwise in 100 steps and the difference between the rotated angle and orientation angle detected through eq. (5) is calculated.

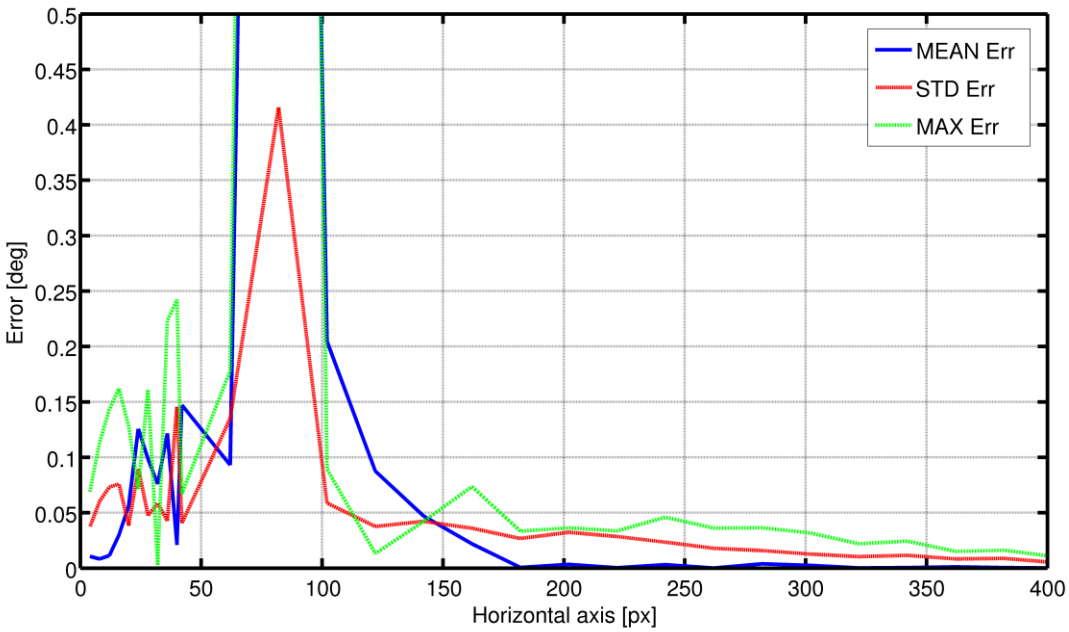

Figure 4. *Precision of orientation determination for several elliptic targets. One axis of the ellipse has been fixed to 80 px while the other has been changed to different lengths. Lines represent the mean error in determining the orientation, the standard deviation and the maximum error.*

Results show that we are able to detect rotations up to 0.025 degrees for very eccentric ellipses. If we read the graph from right to left, we can see that, as the ellipse becomes more and more circular the error slowly increases. For ellipses whose eccentricity is below 0.75 (approximately between 50 and 120 px), the error increases very fast and fails for the exact circle (eccentricity equal to zero), since the orientation angle is not well defined for this case and the obtained angular value is not reliable. For axis lengths shorter than 50 px, the ellipse is too small and, as it happened in the circular target, the error presents a rough profile.

For the sake of completeness, we have evaluated the mean squared error (MSE) of all ellipse fittings, i.e. MSE of the distance between the real ellipses and the fitted ones. For ellipses whose major axis was above 120 px, the MSE resulted below 1.5×10^{-4}px. In the case of the circle and the simulation of target location, the value was even lower than 0.5×10^{-4}px for diameters larger than 160 px. In ideal tests like those here presented, the MSE does not provide important information; however, in real cases, sudden increases of this parameter may show a distortion in the shape, which maybe caused by errors in the target extraction from the scene. Low MSE guarantees the reliability of the process.

4. Experimental results

In order to check the real performance of our proposal, two experiments are proposed. In one case, the target is attached to a rotating plate (see figure 5a). The position of the ellipse is eccentric, so it makes a compound movement consisting of a translation around plate center and a rotation around the ellipse center. The plate rotates at 18.12 arcsec/s. The camera was placed at 2 m from the target thus providing an ellipse image size of 45×106pixels and a resolution of 0.903 px/mm.

In the second case, the target is placed perpendicularly to the plate and rotates around its vertical meridian, thus changing its projected shape onto the image plane (Figure 5b). In both cases, the sequences have been captured with an AOS X-PRI high-speed camera. The image processing is done off-line and frame-per-frame, being the calculation time of 10 ms per frame.

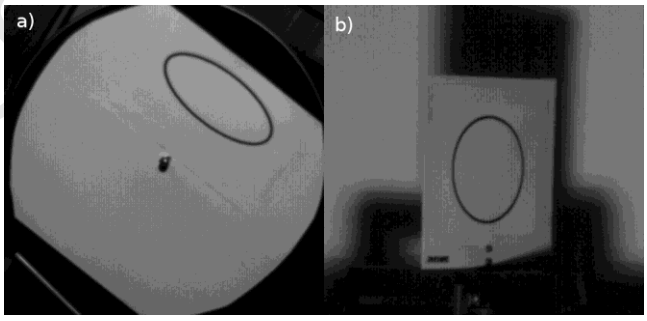

Figure 5. *Targets used in the experiments. a) Ellipse rotates around the fixed central point thus making a movement of translation and rotation. b) Ellipse rotates around its vertical axis thus changing its shape due to the projection onto the image plane.*

The elliptical target contour must be extracted from the image in order to obtain the main geometrical parameters through equations (2-4). The general procedure is as follows: first the background is removed through a high aperture median filter and substracting the result to the original image. Then, the scene is binarized to a convenient level. Noise and blobs in the image are removed through morphological filters [16] until the target is clearly seen as a clear line. Frame processing starts by manually selecting a seed-point inside the ellipse in the first frame. From the gray values around this point, a threshold is calculated and the image is binarized. The line surrounding this seed point is detected and extracted through mathematical morphology boundary tracing [15]. These line points are fitted to equation (1), thus obtaining the ellipse parameters (eq. 2 to 4). The center of the each ellipse is used as the seed -point for the following frame so the remaining processing is automatic. Finally, the obtained values are fitted to their respective expected values. The experimental accuracy of the method is determined by three times the standard deviation of the fitting residuals.

The obtained mean and standard deviation value of all the ellipse fittings of a sequence is $(1.3 \pm 0.2) \times 10^{-3}$px. This error is one order of magnitude higher than the MSE obtained in the simulation for an equivalent ellipse and it is mainly due to the thickness of the ellipse line. In the numerical simulations, the targets were only one pixel wide while, here, the thickness depends on the threshold level. It has been checked that changing the threshold affects to the MSE but it does not significantly influence on the value of the obtained parameters, although it may increase the dispersion [17].

In figure 6, we represent the coordinates of the ellipse center obtained through the full sequence. In order to facilitate representation and direct comparison, we depict the difference from their mean value. According to the translation movement, the center coordinates (X_c, Y_c) follow a trajectory in the form $(A\cos(\omega\alpha + \phi), A\sin(\omega\alpha + \phi))$, where A corresponds to the rotation radius and α is the angle where the ellipse centre should to be located, which can be easily determined from the rotating speed and a cronometer. If the ellipse is correctly located, ω and ϕ

should theoretically be equal the one and zero, respectively. Least square fittings of both coordinates to the trajectory provide the following values, where the 95% confidence bounds are given between in parentheses:

$$\begin{array}{rll} & A = 67.84px & (67.83,67.84) \\ X_c \rightarrow & \omega = 0.99924 & (0.99924,0.99925) \\ & \phi = -2.48435º & (-2.49179, -2.47690) \end{array}$$

$$\begin{array}{rll} & A = 67.80px & (67.80,67.81) \\ Y_c \rightarrow & \omega = 0.99867 & (0.99867,0.99934) \\ & \phi = -2.58977º & (-2.58978, -2.58977) \end{array} \quad (5)$$

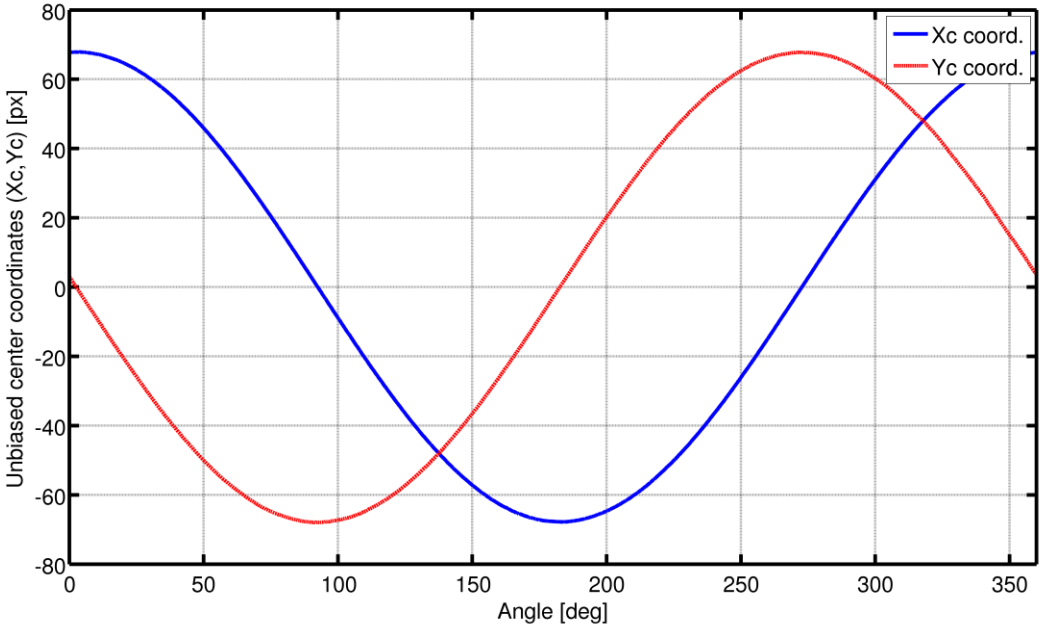

Figure 6. *Computed position of the ellipse center with respect to its azimuthal position. Depicted values are variations with respect to the mean position* $(\bar{X}_c, \bar{Y}_c) = (402.996,291.291)$

The correlation coefficient for both fittings has been equal to one, while the residuals have been (mean ± standard deviation): -0.010 ± 0.059 px, for X_c, and -0.002 ± 0.059 for Y_c. The correspondence between results for both coordinates shows the consistency of the method. The values obtained for ϕ only show a zero error that can be corrected by a re-calibration of the

system. The values obtained for ω and the narrowness of the confidence intervals also show the reliability of the method. The obtained small residuals prove that the method is able to locate the target with high accuracy.

The second parameter analyzed with this experiment was the orientation of the ellipse. The orientation angle is linked to the translation movement, so it can be related to the expected azimuthal postion of the target according to the trajectory equation. Fitting of the computed orientation angle of the ellipse, *y*, to the angular position of the target α, provides:

$$y = m\alpha + n$$

$$\begin{matrix} m = 0.9991(0.9989,0.9992) \\ n = 0.1527(0.1491,0.1563) \end{matrix} \quad (6)$$

$$r^2 = 1$$

Residuals were also calculated giving an average value of 0.000 ± 0.039 degrees. Results show the reliability of the method in determining the orientation of the ellipse.

Just for completeness, we have calculated the major and minor axes. Since the target shape does not change throughout the experiment, we expect that those values are stable. The indetermination in the value of the semi-axis gives information about the subpixel accuracy in detecting the shape of the ellipse. Following (3), the fittings provides as mean values in pixels:

$$\begin{matrix} a = 105.60 \pm 0.15 \\ b = 45.53 \pm 0.08 \end{matrix} \quad (7)$$

These results are in accordance with the shape of the ellipse on the image plane: (106×45) px.

The second experiment was conducted to prove the reliability of the method in detecting rotations outside the image plane (Figure 5b). The rotation speed was the same than in the previous case (18.12 arcsec/s). The camera was situated 2.5 m far from the target, the image resolution was 0.801 px/mm and the image circle diameter was 68 px.

Frame processing is performed as in the previous experiment. An important problem that arises with this experimental performance is that the illumination on the image plane changes with projection, and also does the contrast. In our particular case, we used a frontal illumination with halogen lamp of 500 W. The sequence was recorded at 500 fps, since higher rates did not allow distinguishing the target rotated from the frontal position. As we said above, image processing consisted on an image thresholding followed by a binary boundary tracing. By stating the threshold level relative to the target background minimum luminance in each frame, one can eliminate the effects of the low contrast (up to a limit) since the line will be always darker.

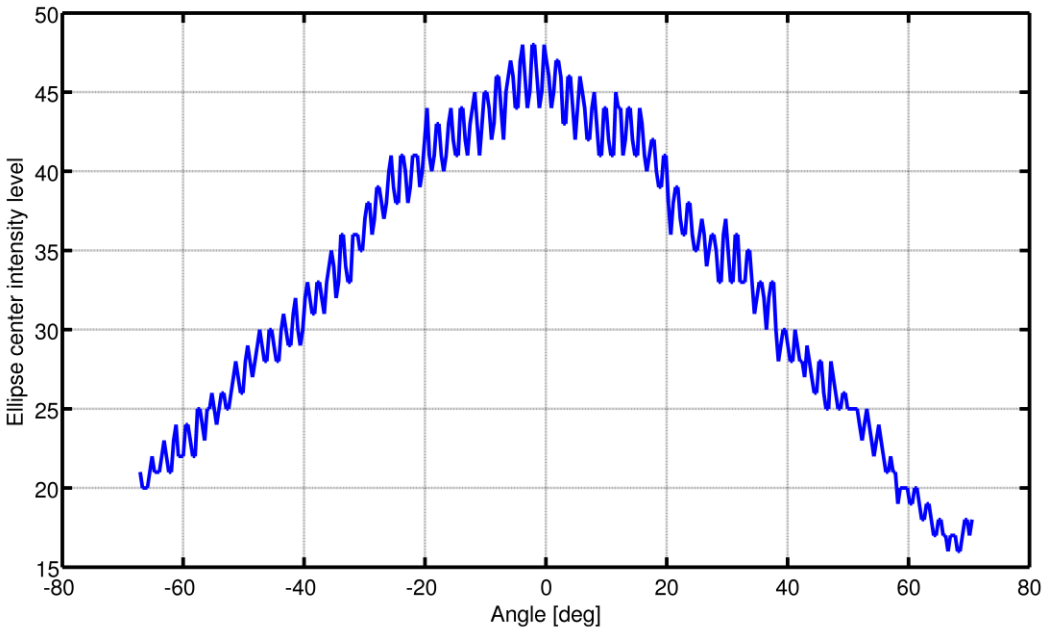

Figure 7. *Brightness variation of the ellipse center with respect to the orientation angle. Zero angle means that the target is perpendicular to the camera axis.*

In figure 7, we represent the gray level of the ellipse center through the whole sequence. We can see there the strong changes in the illumination with the object orientation. Fast oscillations are produced by the illuminating lamp, which was connected to a standard AC source (100 Hz). Although a full half cycle was recorded, we were only able to obtain reliable results in the range from -65º to 65º approximately.

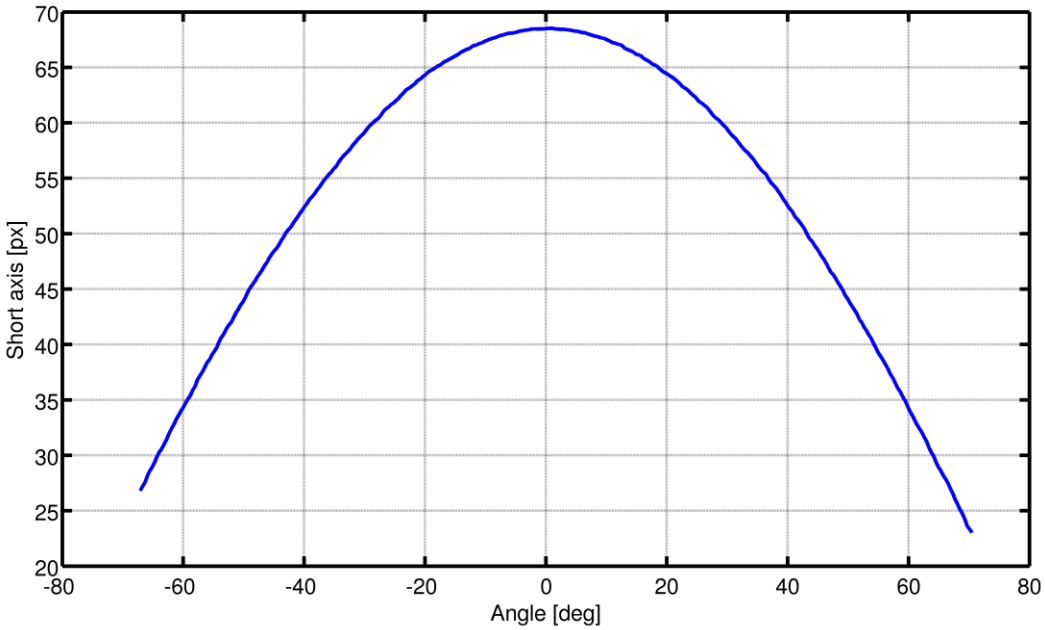

Figure 8. *Measured variation of the short axis with respect to the target orientation. Zero angle means that the target is perpendicular to the camera axis.*

We have evaluated again the main geometrical parameters. Regarding the MSE of the ellipse in the interval [-20º, 20º] is $(1.0 \pm 0.2) \times 10^{-3}$px. Although the data set is very noisy, this value tends to increase with the projection angle so that the MSE for the whole interval [-65º,65º] results to be $(2.0 \pm 0.3) \times 10^{-3}$px. In any case, these values are in concordance with those obtained in the previous experiment. Since the rotation occurs around the vertical axis, the evaluated long axis remained stable, with an average value of 68.5 ± 0.1 px. Regarding the short axis depicted in figure 8, and according to the image projection, it changes following a cosine law in the form:

$$b = A\cos(\omega\alpha + \phi) \tag{8}$$

A is the maximum size of the projection. Since the target rotates around the vertical meridian, this parameter will coincide with the circle diameter. α is the rotation angle, which is given from the rotating speed and the time ,and thus, as previously, ω should be equal to one. Finally, ϕ is

the zero error for the frontal position. Least square fitting to (8) of the obtained values for the short axis gives:

$$\begin{array}{ll} A = 68.47px & (68.46,68.49) \\ \omega = 0.9992 & (0.9987,0.9992) \\ \phi = -0.0529º & (-0.0656,-0.0402) \end{array} \quad (9)$$

The correlation coefficient for this fitting has been 1, while the mean residual and standard deviation is 0.00 ± 0.09 px.

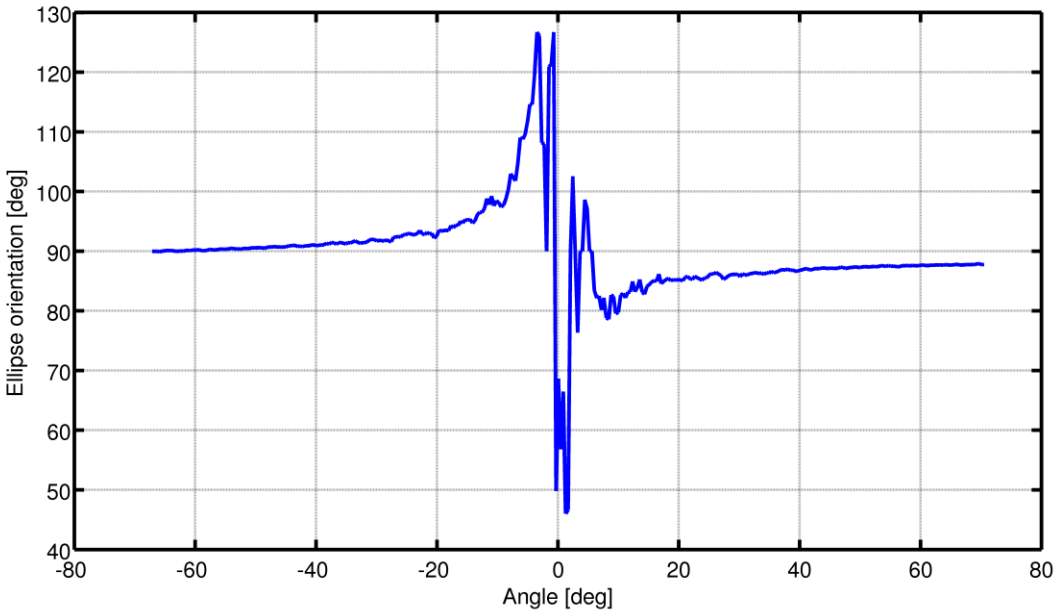

Figure 9. *Variation of the ellipse orientation with respect to the target orientation. Zero angle means that the target is perpendicular to the camera axis.*

Regarding the in-plane orientation angle of the ellipse plotted in figure 9, the graph presents an erratic behavior around 0 degrees with the target at the frontal position, where it is circular shaped. The problems in detecting the angle appear in the range [-30º,30º], with values of eccentricity above 0.5. This result is worse than the one obtained in the numerical analysis (figure 3) and show a practical limit on the ellipse shape for target rotation detection.

By assuming that the obtained tracking error is assimilated to three times the standard deviation of the calculated residuals, the error is about one order of magnitude larger than that obtained in the equivalent numerical case: 0.2 px in position, 0.1º in orientation and 0.3 px for axis length determination. This may be a direct consequence of the MSE of the ellipse fitting: the more inaccurate the ellipse is calculated, the worse results are obtained. In any case, these error estimations are very conservative and can be further improved depending on the particular experimental implementation. Nevertheless, it results obvious for us that the proposed technique is able to accurately track ellipse movements in five degrees of freedom. Although some limitations have been pointed out, these can be easily overcome by a proper target design.

5. CONCLUSIONS

In this paper, we have presented a method for planar object tracking with high-speed video cameras. The use of contour-based methods avoids the influence of noise and irregular illumination on the target. Additionally, knowledge of target geometry allows comparison of the captured with the original shape target and infer its position in five degrees of freedom: localization in the image plane and orientation in the three-dimensional space. Movements of the object along the camera axis are not detectable while the movement does not produce a change in the target size. In our particular case, the target has elliptical shape, since it is easy to recognize and track.

Different numerical tests have been performed in order to determine the accuracy of the method. We have evaluated the sensitivity of the method in determining the center, orientation and axis lengths of the ellipse. Numerical results have been validated through two experiments that show the real performance of the method. In the first one, an ellipse is tracked while it rotates around a fixed point and around its own center. Both movements are detected and correctly described with subpixel accuracy. In the second experiment, we track the position of the ellipse as it rotates around an axis perpendicular to the camera optical axis.

Experiments show that we are able to increase the nominal resolution of the digital sensor in at least one order of magnitude. Notice also that no previous calibration of the imaging setup has

been done, since all detected changes are relative. If one is interested in obtaining absolute values of displacement/rotation, the real size of the target should be used in order to obtain the pixel to millimeter conversion. Apart of this conversion, and while the target shape is not optically distorted, no additional considerations are needed.

Regarding the potential applications of the technique, we are interested in applying the technique for tracking structural vibrations [11] where a planar target can be easily attached and the movements are, somehow, restricted. In those cases, target may receive direct daylight, which is unstable due to the presence of clouds, changing angle of the sun and uncontrolled presence of shadows. The use of contour based methods guarantees that the target can be tracked with independence of the illumination. Other found applications deal with detection of fast ocular movements [2]. In that case, the eye-pupil can be considered planar and its movement is restricted. Under infrared illumination, the pupil limits can be clearly established thus making possible the use of the method here presented.

ACKNOWLEDGMENTS

The authors acknowledge the support of the Spanish Ministerio de Economía y Competitividad through the project BIA2011-22704 and the Generalitat Valenciana through the projects GV/2013/009 and PROMETEO/ 2011/021. A. B. Roig acknowledges a grant from Cajamurcia

REFERENCES

[1] J.J. Lee, M. Shinozuka, “A vision based system for remote sensing of bridge displacement” NDT&E International 39 (2006) 425-431

[2] A.B. Roig, M. Morales, J. Espinosa, J. Perez, D. Mas, C. Illueca, “Pupil detection and tracking for analysis of fixational eye micromovements” Optik 123, (2012) 11-15.

[3] D. Mas, B. Ferrer, J. T. Sheridan, J. Espinosa, “Resolution limits to subpixel accuracy” Opt. Letters, 37 (2012) 4877-4879.

[4] M.R. Shortis, T.A. Clarke, T.A. Short, “A comparison of some techniques for the subpixel location of discrete target image” Proc. SPIE 2350 (1994) 230-250.

[5] M.R. Shortis, T.A. Clarke, S. Robson, " Practical testing of the precision and accuracy of target image centring algorithms" Proc. SPIE 2598, (1995) 65-75

[6] A.M. Bruckstein, A. O'Gorman, "Design of shapes for precise Image registration" IEEE T. Inform. Theory, 44, (1998) 3156-3162.

[7] J.C. Trinder, J. Jansa, Y. Huang, "An assessment of the precision and accuracy of methods of digital target localization" ISPRS J. Photogramm. 50 (1995) 12-20.

[8] I. Maalen-Johansen, "On the precision of subpixel measurements in videometry" Proc SPIE 2252 (1993), 169–178.

[9] W. Tong, "Subpixel image registration with reduced bias" Opt. Lett. 36, (2011) 763-765 .

[10] J.O. Otepka, C.S. Fraser, "Accuracy enhancement of vision metrology through automatic target plane determination" Proceedings of the ISPRS Congress (2004), Part B, 873-879.

[11] B. Ferrer, J. Espinosa, J. Perez, S. Iborra, D. Mas, "Optical scanning for structural vibration measurement" Res. Nondestruct. Eval. 22, (2011) 61-75.

[12] C.C. Chang, X.H. Xiao, "An integrated visual-inertial technique for structural displacement and velocity measurement" Smart Struct. Syst. 6 (2010) 1025-1039.

[13] T.A. Clarke, X. Wang, "Extracting high precision information from CCD images". Proc. ImechE Conf., Optical methods and data processing for heat and fluid flow. City University, (1998) 311-320.

[14] O. Gal, in http://www.mathworks.com/matlabcentral/fileexchange/3215-fitellipse last seen in 04-12-2011

[15] L. O'Gorman, A. W. Bruckstein, C. B. Bose, I. Amir, "Subpixel registration using a concentric fiducial" Proc. 10Th Int. Conf. Pattern Recognition, 249-253., Atlantic City, 1990.

[16] J. Serra, *"Image Analysis and Mathematical Morphology"* Academic Press, Inc., (Orlando, FL, 1983).

[17] D. Mas, J. Espinosa, A. B. Roig, B. Ferrer, J. Perez, C. Illueca "Measurement of wide frequency range structural microvibrations with a pocket digital camera and sub-pixel techniques" Appl. Opt. 51 (2012) 2664-2671.